XLI CILAMCE
XLI Ibero-Latin American Congress on Computational Methods in Engineering
16-19 November, 2020 FOZ DO IGUAÇU PARANÁ - BRAZIL

Simulation of a drop impact on a moving wall with a liquid film using the convected level-set method

Malú Grave[1], Jose J. Camata[2], Alvaro L. G. A. Coutinho[1]

[1]*Dept. of Civil Engineering, COPPE/Federal University of Rio de Janeiro*
P.O. Box 68506, RJ 21945-970, Rio de Janeiro, Brazil
malugrave@nacad.ufrj.br, alvaro@nacad.ufrj.br
[2]*Dept. of Computer Science, Federal University of Juiz de Fora*
Campus Universidade Federal de Juiz de Fora, Via Local, 4569, MG 36036-900, Juiz de Fora, Brazil
camata@ice.ufjf.br

Abstract. A liquid drop impact on a moving wall with a pre-existing thin film of the same liquid is simulated using the convected level-set method. We couple this interface-capturing method with the Navier-Stokes equations, and we apply a global mass conservation procedure to enforce the mass balance between phases. The analysis takes into account viscous, inertial, and surface tension forces, neglecting gravity. The Continuum Surface Force (CSF) approach models surface tension forces. We solve the Navier-Stokes equations with the residual-based variational multiscale finite element formulation and the convected level-set with a SUPG formulation with discontinuity-capturing. We implement the whole model in libMesh, an open finite element library that provides a framework for multiphysics, considering adaptive mesh refinement. The values of the Reynolds and Weber numbers determine different drop splash regimes. Numerical results are presented for 2D and 3D liquid drop impacts, and they are in good agreement with other simulations.

Keywords: Drop splashing, Moving wall, Two-phase flow, Level-set

1 Introduction

The drop impact on a solid or liquid surface is a common phenomenon that occurs in many situations. These include industrial applications such as welding in material processing, coating, painting, cooling, fuel injection in internal combustion engines; also ink-jet printing, agricultural aspects related to the rainfall as soil erosion, among others [1–4]. An understanding of the physics of drop impact on wet walls is essential in optimizing these applications. The physical phenomena accompanying drop impact on a surface have fascinated researchers for a long time because of their intrinsic complexity and practical importance. It comprises a wide variety of fluid mechanics facets, such as multiphase and interfacial flows. Various numerical methods have been applied to simulate such flows, including the Volume of Fluid (VOF) method [5], the Front Tracking Method (FTM) [6], the Lattice Boltzmann Method (LBM) [7], the Smoothed Particle Hydrodynamics (SPH) [8], the Phase Field method [9], and the Level-Set method [10].

In this paper, we employ a modified level-set method that associates both re-initialization and convection steps. The method is called convected level-set [11, 12]. The inclusion of the re-initialization in the convection equation avoids the extra step appearing in the original level-set formulation. Based on [10] and the CLS methods [13, 14], we introduced [15] a new truncated signed distance function to get a smooth truncation far from the interface and improve the mass conservation. This method is coupled with the Navier-Stokes equations, which are discretized by the residual-based variational multiscale finite element formulation. Moreover, we consider adaptive mesh refinement based on the flux jump of the level-set errors in our simulations. All implementations in this work uses the `libMesh` library. `libMesh` is an open-source library that provides a platform for parallel, adaptive, multiphysics finite element simulations [16]. The main advantage of `libMesh` is the possibility to focus on the implementation of the modeling specific features without worrying about issues such as adaptivity and code parallelization. Consequently, it tends to minimize the effort to build a high performance computing code.

The objective of this study is to represent the drop impact on a moving wall with a liquid film. The remainder of this paper is organized as follows. We start in section 2 with a description of the problem of interest. Then, we

present the convected level-set method and the new truncated signed distance function. In section 4, we present the Navier-Stokes equations for two-phase flows. Section 5 provides the validation of our model and the results obtained. Finally, the paper ends with a summary of our main conclusions.

2 Problem Description

Figure 1 depicts a sketch showing the main parameters of the problem of a droplet impact on a moving plane wall with a thin liquid film.

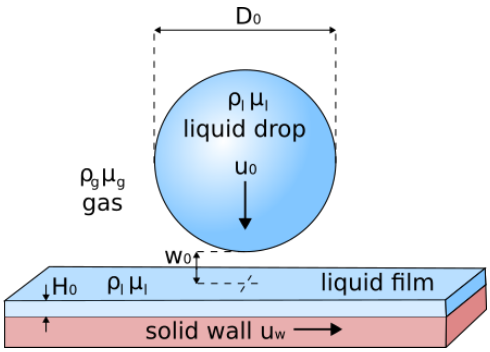

Figure 1. Schematic sketch of a droplet impact on a moving plane wall with a thin liquid film.

We consider that a liquid drop of diameter D_0, density ρ_l, and dynamic viscosity μ_l normally impacts onto a wall with a thin liquid film of the same liquid, with an impact velocity u_0. The thickness of the film is H_0. The surrounding gas has density ρ_g and viscosity μ_g. The liquid–gas surface tension is σ_{st}. The drop is initially placed at a distance $z_0 = 0.5D_0 + H_0 + w$ from the wall; here, the interface width $w_0 = 0$. At that stage of drop splashing, gravity effects are typically not important [17, 18]. Therefore, we neglect gravity in the present study. The computational domain is $l_x \times l_y \times l_z$, where l_x and l_y are the lateral dimensions of the domain in the horizontal direction, and l_z is the dimension in the vertical direction. The no-slip boundary condition is used at $z = 0$, while pressure boundary conditions are applied at $z = l_z$. Open boundary conditions are used at the rest of the boundaries. The initial velocity field is,

$$\mathbf{u} = \begin{cases} -u_0\mathbf{k}, \ (\rho = \rho_l, z > 0) \\ u_w\mathbf{i}, \ (\rho = \rho_l, z \leq 0) \\ 0, \ (\rho = \rho_g) \end{cases} \tag{1}$$

To model this problem, we couple a new convected level-set method with the Navier-Stokes equations. The governing equations are explained in the following sections.

3 Convected Level-Set Method

The level-set method was first introduced by Osher and Sethian [19] in the late 1980s as a technique for capturing evolving interfaces and tracking the propagation of fronts. In this work, we applied a modified level-set method to track the movement of the interface between the liquid and gas phases. The method consists in to separate two phases with signed distance functions (SDFs), in which the zero level-set defines the interface between phases. Here, following [15], we introduce a new modified SDF (ϕ), inspired in [10], given by,

$$\phi = \frac{1}{1 + e^{\frac{-\alpha}{E}}} - 0.5 \tag{2}$$

in which the parameter E defines the thickness where the modified SDF is distributed and α is the standard level-set function given by,

$$\alpha(\mathbf{x}) = \begin{cases} d(\mathbf{x}, \Gamma) \text{ for } \mathbf{x} \in \Omega^+ \\ 0 \text{ for } \mathbf{x} \in \Gamma \\ -d(\mathbf{x}, \Gamma) \text{ for } \mathbf{x} \in \Omega^-. \end{cases} \tag{3}$$

In this work, we define $E = 2h_e$, with h_e being the mesh size. The bigger the value of E, the smoother is the transition between phases. However, as in the CLS methods [13, 14], we would like a sharp transition to improve mass conservation. The idea is to minimize this region as much as possible and still have a smooth transition between phases. The truncated level-set function verifies the following property,

$$S = ||\nabla\phi|| = \frac{1}{4E} - \frac{\phi^2}{E}. \tag{4}$$

The convected level-set method avoids the re-initialization step of the original formulation by combining the re-initialization with the convection equation in one single equation [11, 12, 15, 20]. Thus, the interface motion is given by the following resulting equation,

$$\begin{aligned} \frac{\partial\phi}{\partial t} + (\mathbf{u} + \lambda\mathbf{U})\cdot\nabla\phi - \lambda\,\mathrm{sgn}(\phi)\left(\frac{1}{4E} - \frac{\phi^2}{E}\right) = 0 \\ \phi(t=0,\mathbf{x}) = \phi_0(\mathbf{x}). \end{aligned} \tag{5}$$

where $\mathbf{U} = \mathrm{sgn}(\phi)\dfrac{\nabla\phi}{||\nabla\phi||}$, λ is a penalty constant and sgn is the sign function.

4 Navier-Stokes Equations

The Navier-Stokes equations govern the fluid flow. In this work, the effects of gravity are neglected, and we present the dimensionless form of the Navier-Stokes equations, which lead to the following nonlinear mathematical problem to be solved: let us consider a space-time domain in which the flow takes place along the interval $[0, t_f^*]$ given by $\Omega \subset R^{n_{sd}}$, where n_{sd} is the number of space dimensions. Let $\overline{\Gamma}$ denote the boundary of Ω. Find the pressure p^* and the velocity $\mathbf{u}^*$ satisfying the following equations,

$$\rho^*\frac{\partial\mathbf{u}^*}{\partial t^*} + \rho^*\mathbf{u}^*\cdot\nabla\mathbf{u}^* + \nabla p^* - \frac{1}{Re}\nabla\cdot(\mu^*\nabla\mathbf{u}^*) - \frac{\mathbf{F}_{\mathbf{st}}^*}{We} = 0 \text{ in } \Omega\times[0,t_f] \tag{6}$$

$$\nabla\cdot\mathbf{u}^* = 0 \text{ in } \Omega\times[0,t_f]. \tag{7}$$

where ρ^* is the density, μ^* is the dynamic viscosity and $\mathbf{F_{st}}^*$ is the surface tension force. The superscript $*$ indicates that the parameters are in the dimensionless form. The dimensionless variables and parameters are given by,

$$Re = \frac{\rho_l u_0 D_0}{\mu_l} \tag{8}$$

$$Fr = \frac{u_0}{\sqrt{||\mathbf{g}||D_0}} \tag{9}$$

$$We = \frac{\rho_l u_0^2 D_0}{\sigma_{st}} \tag{10}$$

$$\mathbf{x}^* = \frac{\mathbf{x}}{D_0} \tag{11}$$

$$t^* = \frac{u_0}{D_0}t \tag{12}$$

$$\mathbf{u}^* = \frac{\mathbf{u}}{u_0} \tag{13}$$

$$\rho^* = \frac{\rho}{\rho_l} \tag{14}$$

$$\mu^* = \frac{\mu}{\mu_l} \tag{15}$$

$$\mathbf{F_{st}}^* = \frac{\mathbf{F_{st}}}{\sigma_{st}}. \tag{16}$$

where σ_{st} is the surface tension coefficient.

To represent the heterogeneous flow material properties, such as the density ρ and the dynamic viscosity μ, we introduce the following mixing laws, that depends on the SDF function,

$$\rho = \rho_l\mathcal{H}_{scaled}(\alpha) + \rho_g(1 - \mathcal{H}_{scaled}(\alpha)) \tag{17}$$

$$\mu = \mu_l\mathcal{H}_{scaled}(\alpha) + \mu_g(1 - \mathcal{H}_{scaled}(\alpha)) \tag{18}$$

where $\mathcal{H}_{scaled}$ is a non-symmetrical, smoothed Heaviside function [21].

The surface tension force is applied using the Continuum Surface Model (CSF) [22], that is,

$$\mathbf{F_{st}} = \sigma_{st}\kappa\mathbf{n}\delta(\phi) \tag{19}$$

κ is the curvature, $\mathbf{n}$ is the normal vector to the interface and $\delta(\phi)$ is a delta function where the surface tension is distributed and satisfies $\delta(\phi) = \frac{\partial\mathcal{H}}{\partial\phi}$. An advantage of an SDF is that the normal vector to the interface and the curvature can be approximated as,

$$\mathbf{n} = \nabla\phi \tag{20}$$

$$\kappa(\phi) = \nabla \cdot \frac{\nabla\phi}{||\nabla\phi||}. \tag{21}$$

Note that in the dimensionless analysis, there is no need to know the value of the surface tension if the Weber number is provided, since the dimensionless surface tension force may be written as $\mathbf{F}^*_{\mathbf{st}} = \kappa\mathbf{n}\delta(\phi)$. To approximate the Navier-Stokes equations, we use a finite element Residual-Based Variational Multiscale Formulation (RBVMS). Detailed reviews of the RBVMS formulation are in [23–26]. See [15] for a complete description of the equations and methods used in this work.

5 Results and Discussion

In this section, we will assess the accuracy and performance of the numerical method by solving some representative problems. First, we validate the code by simulating 2D and 3D droplet impact on a stationary wall. Then, we study the effects of the drop impact on a moving wall.

5.1 2D validation of droplet impact on a stationary liquid film

First, we validate our code by simulating a droplet impact on a stationary liquid film with large density ratio and high Reynolds numbers in a 2D domain. In this case, the wall is fixed, i.e., $u^*_w = 0$. The liquid film height is defined as $H^* = 0.15$, the diameter $D^*_0 = 1$ and the impact velocity $u^*_0 = 1$. The dimensions of the computational domain are $[10 \times 2.5]$. We set $\rho_l/\rho_g = 10^3$ and $\mu_l/\mu_g = 10^2$. Three simulations at different Reynolds numbers have been carried out ($Re = 20$, $Re = 100$ and $Re = 1000$). The Weber number is set as $We = 2000$ in all simulations. Figures 2, 3 e 4 show the simulations snapshots at different time-steps. Similar observations were reported in the work of [27] and [10].

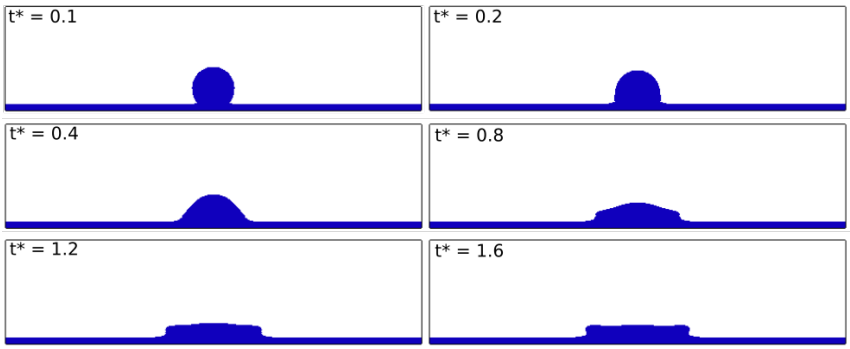

Figure 2. Time evolution of droplet splashing on a thin film at Re = 20, We = 2000.

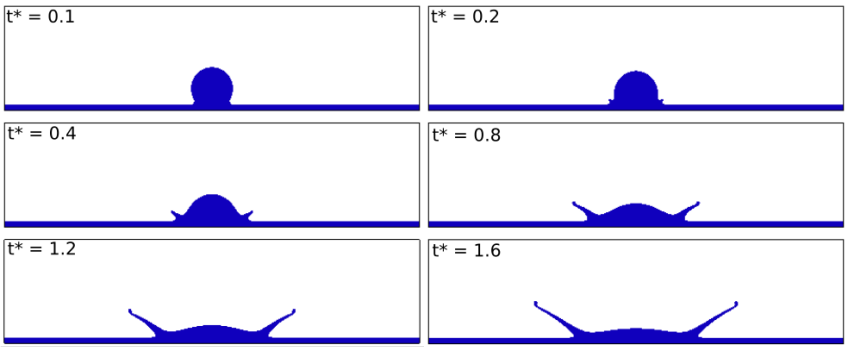

Figure 3. Time evolution of droplet splashing on a thin film at Re = 100, We = 2000.

5.2 3D validation of droplet impact on a stationary liquid film

To further validate our code, we simulate a 3D case of a drop splashing on a stationary thin liquid film. We consider $u_w = 0$, $We = 300$, $Re = 2000$, $H^* = 0.15$, $D^*_0 = 1$ and $u^*_0 = 1$. The dimensions of the computational

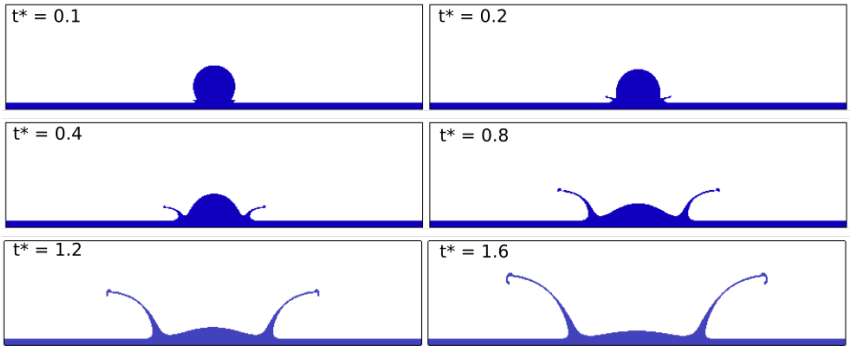

Figure 4. Time evolution of droplet splashing on a thin film at Re = 1000, We = 2000.

domain are $[6 \times 6 \times 3]$. We set $\rho_l/\rho_g = 100$ and $\mu_l/\mu_g = 50$. The no-slip boundary condition is used at $z = 0$, while pressure boundary conditions are applied at $z = 3$. The periodic boundary conditions are used at the lateral boundaries. Here, we use adaptive mesh refinement. The initial mesh has $30 \times 30 \times 15$ trilinear hexahedral elements, and after the refinement, the smallest element has size 0.025. We compare our results with [7], which used a mesh five times more refined than our smallest element. Figure 5 shows two snapshots of both results, and it is possible to see that the behavior is quite similar.

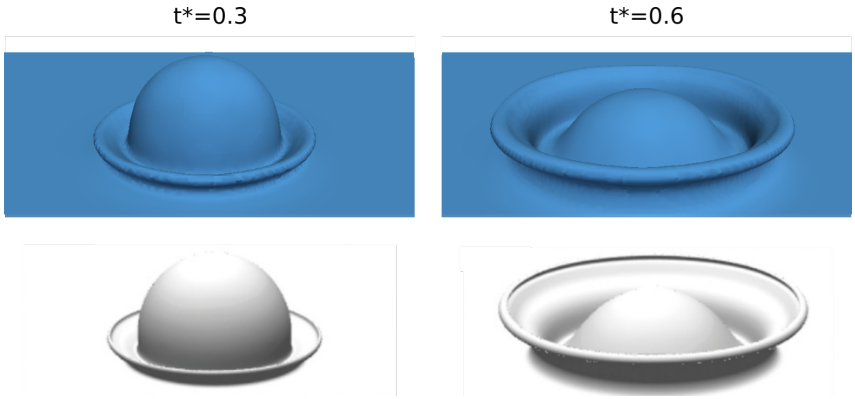

Figure 5. Comparison of the snapshots of a 3D droplet splashing on a stationary thin film. Top: present work. Bottom: results from [7].

5.3 Simulation of a Droplet Impact on a Moving Mall with a Liquid Film

Now, we simulate the normal impact of a liquid drop on a moving wall, which is covered by a thin film of the same liquid. The initial configurations are the same as the previous section, except for the wall velocity, which is different from zero. We present the results considering two wall velocities: $u_w^* = 0.5$ and $u_w^* = 1$. Figure 6 shows snapshots of both simulations, and it is possible to see how the wall velocity affects the drop impact. However, note that the adaptive mesh used in these simulations is still too coarse to capture the fine details of the physics. Mesh refinement is necessary for better results, and it is foreseen for future works.

6 Conclusions

We coupled the convected level-set method with the Navier-Stokes equations to simulate a droplet impact on a moving wall with a thin liquid film. First, we presented results for a 2D simulation of a droplet impact in a stationary wall. We have shown the difference in the behavior of the impact depending on the Reynolds number. Then, we validated the code for 3D simulations by testing a droplet impact on a stationary wall and comparing it with other simulations, with excellent agreement. Finally, we showed the effects of a moving wall. The results are qualitative because the mesh refinement is too coarse to reproduce the fine details of this problem. As future work, we will perform a grid convergence study, to find the ideal refinement.

Another critical question that was not considered in this work is the fact that in real flows, once the drop impacts the surface, instability takes place immediately after the impact. This instability may grow with time and

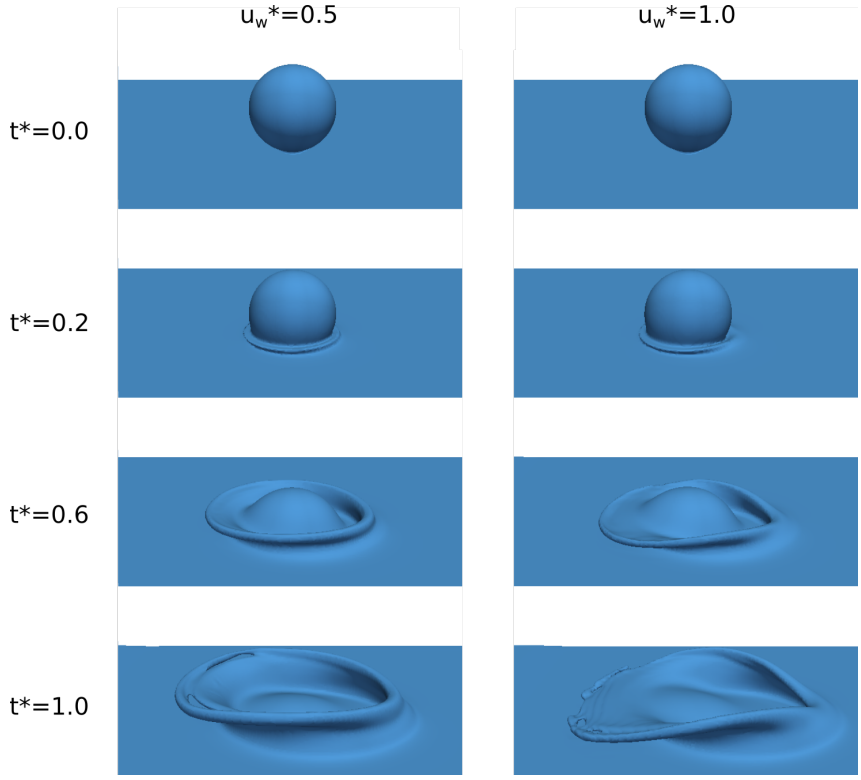

Figure 6. Snapshots of a 3D droplet splashing on a moving wall with a liquid film.

eventually causes a crown spike formation. Therefore, an initial perturbation is required to represent the instability in numerical simulations. We propose to consider this as future work as well.

Acknowledgements. This study was financed in part by the Coordenação de Aperfeiçoamento de Pessoal de Nível Superior- Brasil (CAPES) - Finance Code 001. This work is also partially supported by CNPq, FAPERJ, ANP and Petrobras.

Authorship statement. The authors hereby confirm that they are the sole liable persons responsible for the authorship of this work, and that all material that has been herein included as part of the present paper is either the property (and authorship) of the authors, or has the permission of the owners to be included here.

References

[1] Chinakhov, D., 2013. Calculation of gas-dynamic impact of the active shielding gas on the electrode metal drop in gas jet shielded welding. In *Applied Mechanics and Materials*, volume 379, pp. 188–194. Trans Tech Publ.
[2] Moreira, A., Moita, A., & Panao, M., 2010. Advances and challenges in explaining fuel spray impingement: How much of single droplet impact research is useful? *Progress in energy and combustion science*, vol. 36, n. 5, pp. 554–580.
[3] Derby, B., 2011. Inkjet printing ceramics: From drops to solid. *Journal of the European Ceramic Society*, vol. 31, n. 14, pp. 2543–2550.
[4] Joung, Y. S. & Buie, C. R., 2015. Aerosol generation by raindrop impact on soil. *Nature communications*, vol. 6, n. 1, pp. 1–9.
[5] Gunjal, P. R., Ranade, V. V., & Chaudhari, R. V., 2005. Dynamics of drop impact on solid surface: experiments and vof simulations. *AIChE Journal*, vol. 51, n. 1, pp. 59–78.
[6] Muradoglu, M. & Tasoglu, S., 2010. A front-tracking method for computational modeling of impact and spreading of viscous droplets on solid walls. *Computers & Fluids*, vol. 39, n. 4, pp. 615–625.
[7] Ming, C. & Jing, L., 2014. Lattice boltzmann simulation of a drop impact on a moving wall with a liquid film. *Computers & Mathematics with Applications*, vol. 67, n. 2, pp. 307–317.
[8] Yang, X. & Kong, S.-C., 2018. 3d simulation of drop impact on dry surface using sph method. *International Journal of Computational Methods*, vol. 15, n. 03, pp. 1850011.

[9] Zhang, Q., Qian, T.-Z., & Wang, X.-P., 2016. Phase field simulation of a droplet impacting a solid surface. *Physics of Fluids*, vol. 28, n. 2, pp. 022103.
[10] Bahbah, C., Khalloufi, M., Larcher, A., Mesri, Y., Coupez, T., Valette, R., & Hachem, E., 2019. Conservative and adaptive level-set method for the simulation of two-fluid flows. *Computers & Fluids*, vol. 191, pp. 104223.
[11] Coupez, T., 2007. Convection of local level set function for moving surfaces and interfaces in forming flow. In *AIP Conference Proceedings*, pp. 61–66. AIP.
[12] Ville, L., Silva, L., & Coupez, T., 2011. Convected level set method for the numerical simulation of fluid buckling. *International Journal for Numerical Methods in Fluids*, vol. 66, n. 3, pp. 324–344.
[13] Olsson, E. & Kreiss, G., 2005. A conservative level set method for two phase flow. *Journal of computational physics*, vol. 210, n. 1, pp. 225–246.
[14] Olsson, E., Kreiss, G., & Zahedi, S., 2007. A conservative level set method for two phase flow ii. *Journal of Computational Physics*, vol. 225, n. 1, pp. 785–807.
[15] Grave, M., Camata, J. J., & Coutinho, A. L. G. A., 2020. A new convected level-set method for gas bubble dynamics. *Computers & Fluids*, vol. 209, pp. 104667.
[16] Kirk, B. S., Peterson, J. W., Stogner, R. H., & Carey, G. F., 2006. libmesh: a c++ library for parallel adaptive mesh refinement/coarsening simulations. *Journal Engineering with Computers*, vol. 22, n. 3, pp. 237–254.
[17] Yarin, A. L., 2006. Drop impact dynamics: splashing, spreading, receding, bouncing.... *Annu. Rev. Fluid Mech.*, vol. 38, pp. 159–192.
[18] Coppola, G., Rocco, G., & de Luca, L., 2011. Insights on the impact of a plane drop on a thin liquid film. *Physics of Fluids*, vol. 23, n. 2, pp. 022105.
[19] Osher, S. & Sethian, J., 1988. Fronts propagating with curvature-dependent speed: algorithms based on hamilton-jacobi formulations. *Journal of Computational Physics*, vol. 79, pp. 12–49.
[20] Touré, M. K. & Soulaïmani, A., 2016. Stabilized finite element methods for solving the level set equation without reinitialization. *Computers & Mathematics with Applications*, vol. 71, n. 8, pp. 1602–1623.
[21] Yokoi, K., 2014. A density-scaled continuum surface force model within a balanced force formulation. *Journal of Computational Physics*, vol. 278, pp. 221–228.
[22] Brackbill, J. U., Kothe, D. B., & Zemach, C., 1992. A continuum method for modeling surface tension. *Journal of Computational Physics*, vol. 100, n. 2, pp. 335–354.
[23] Hughes, T. J. R., Scovazzi, G., & Franca, L. P., 2004. Multiscale and stabilized methods. *Encyclopedia of Computational Mechanics Second Edition*.
[24] Rasthofer, U. & Gravemeier, V., 2017. Recent developments in variational multiscale methods for large-eddy simulation of turbulent flow. *Archives of Computational Methods in Engineering*, pp. 1–44.
[25] Ahmed, N., Rebollo, T. C., John, V., & Rubino, S., 2017. A review of variational multiscale methods for the simulation of turbulent incompressible flows. *Archives of Computational Methods in Engineering*, vol. 24, n. 1, pp. 115–164.
[26] Codina, R., Badia, S., Baiges, J., & Principe, J., 2018. Variational multiscale methods in computational fluid dynamics. *Encyclopedia of Computational Mechanics Second Edition*, pp. 1–28.
[27] Wang, Y., Shu, C., Huang, H., & Teo, C., 2015. Multiphase lattice boltzmann flux solver for incompressible multiphase flows with large density ratio. *Journal of Computational Physics*, vol. 280, pp. 404–423.